



## Characteristic of a $\text{Cs}_2\text{LiLaBr}_6:\text{Ce}$ scintillator detector and the responses for fast neutrons<sup>☆</sup>

Jianguo Qin, Jun Xiao, Tonghua Zhu, Xinxin Lu<sup>\*</sup>, Zijie Han, Mei Wang, Li Jiang, Yunfeng Mou, Junjie Sun, Zhongwei Wen, Xinhua Wang

Institute of Nuclear Physics and Chemistry, China Academy of Engineering Physics, MianYang 621900, China



### ARTICLE INFO

#### Keywords:

CLLB scintillator  
Pulse shape discrimination  
Fast neutron response  
Neutron activation

### ABSTRACT

The elpasolite crystal CLLB is proposed to detect both  $\gamma$ -ray and thermal neutron events with the ability to distinguish them by pulse shape discrimination (PSD) method. Pulse shapes of  $\gamma$ -ray, alpha particle, thermal and fast neutron events were measured and determined that PSD can be performed to separate  $\gamma$ -ray from alpha and thermal neutron events with a Figure of Merit (FoM) 1.23. The  $\gamma$ -ray non-proportional response is less than 2% in the energy region of 59.6 keV–4438 keV. Fast neutron responses for CLLB scintillator were investigated and analyzed using deuterium tritium (DT) reaction neutrons. The activity of 511 keV  $\gamma$ -ray emitted by  $^{78}\text{Br}$  and  $^{80}\text{Br}$  can reach up to  $\sim 0.709 \text{ Bq}\cdot\text{n}^{-1}$ , some high-energy events at 15 MeVee – 18 MeVee were found that generated according to the reaction  $^6\text{Li}(n, \text{T})^4\text{He}$ .

### 1. Introduction

Cerium ( $\text{Ce}^{3+}$ )-doped crystal  $\text{Cs}_2\text{LiLaBr}_6:\text{Ce}$  is one of the elpasolite scintillators that have recently attracted considerable interest for radiation detection [1–4]. It can be used as dual neutron/ $\gamma$ -ray detector and can distinguish between them. This makes it an attractive option in nuclear parameter measurement for the integral experiment [5] and homeland security [1]. Compared with the CLYC crystal, CLLB crystal has higher density of 4.2 g/cc and higher photo yield of 55 000 ph/MeV [6], this makes CLLB has higher  $\gamma$ -ray detection efficiency and better energy resolution [2] than CLYC and significantly better than that of NaI:Tl [7].

Besides the intrinsic radioactive background from Lanthanum-containing scintillator and the actinium contamination [1], the responses of thermal neutron and fast neutron should be investigated clearly before it was used in the neutron/ $\gamma$ -ray mixed fields. Thermal neutron was detected by the  $^6\text{Li}(n, \alpha)\text{T}$  reaction with  $Q$  value of 4.782 MeV, and an electron equivalent energy of  $\sim 3.2$  MeVee was deposited. In addition, fast neutron can also be detected through this nuclear reaction. More importantly, bromine in the  $\text{Cs}_2\text{LiLaBr}_6:\text{Ce}$  crystal has the highest atomic ratio, both  $^{79}\text{Br}$  and  $^{81}\text{Br}$  have considerable fast neutron reaction cross sections [8], and then the short half-life products  $^{78}\text{Br}$  and  $^{80}\text{Br}$  will result in very high  $\gamma$ -ray radioactivity. This is a serious problem for detecting  $\gamma$ -ray energy spectrum.

In order to investigate fast neutron response of the CLLB scintillator detector, pulse shapes formed by  $\gamma$ -ray, neutron and alpha particle,

pulse shape discrimination ability, energy resolution and  $\gamma$ -ray non-proportional response were characterized firstly. Fast neutron responses of  $^6\text{Li}$ ,  $^{79}\text{Br}$  and  $^{81}\text{Br}$  were studied using the deuterium tritium (DT) reaction neutron, and the activation products  $^{78}\text{Br}$  and  $^{80}\text{Br}$  were measured and analyzed using a HPGe detector.

### 2. Experimental methods

The  $\phi 1.5'' \times 1.5''$  right CLLB crystal containing natural lithium was produced by Saint Gobain Crystals, of which  $^6\text{Li}$  abundance is equal to 7.5%. The crystal was directly coupled to a Hamamatsu photomultiplier tube (PMT) (R10601-100), all of which were sealed in aluminum casing. The PMT was biased to  $-750$  V.

Data were acquired using a 4-channel, 10-bit, 1 GHz, USB-based Flash Analog-to-Digital Converter (FADC) with the waveform digitizer DT5751 which manufactured by CAEN. Pulse output from the PMT was digitized directly and the entire waveform was stored on a hard disk via LabVIEW-based control software.

Pulse height (PH) analysis and pulse shape discrimination (PSD) are based on the charge integration method. The PSD factor is usually defined as  $1 - Q_s/Q_l$ , where  $Q_s$  is a short integration window containing the fast rise time duration of the pulse, and  $Q_l$  is a long integration window containing both the fast and the slow components of the pulse [9]. The figure of merit (FoM) associated with PSD performance is defined as  $\text{FoM} = (P_2 - P_1) / (\text{FWHM}_1 + \text{FWHM}_2)$ , where  $P_1$  and  $P_2$  are the mean value of the Gaussian function, FWHM 1 and FWHM 2 are the full width of half maximum of peak 1 and peak 2, respectively [10].

<sup>☆</sup> Project supported by the National Natural Science Foundation of China (Grant No. 11575165 and 11575163).

<sup>\*</sup> Corresponding author.

E-mail address: [xinxinlu@aliyun.com](mailto:xinxinlu@aliyun.com) (X. Lu).

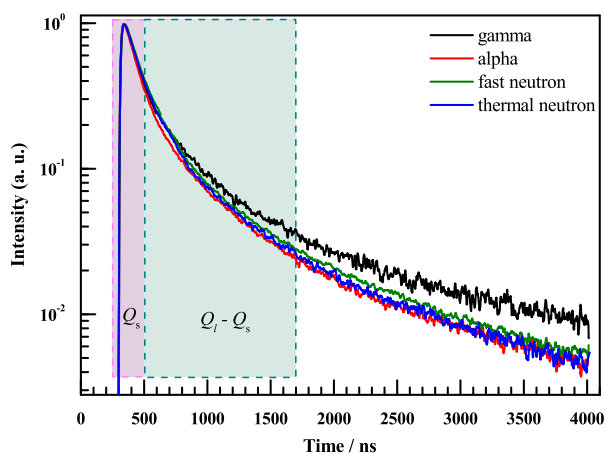


Fig. 1. Waveforms for gamma, alpha, thermal and fast neutron, measured by a  $\Phi 1.5'' \times 1.5''$  right CLLB scintillator and Hamamatsu photomultiplier tube (R10601-100) at  $-750$  V. (Color online).

$\gamma$ -ray and neutron sources were used to investigate the  $\gamma$ -ray, alpha particle and thermal neutron responses, including a set of standard  $\gamma$ -ray sources  $^{22}\text{Na}$ ,  $^{137}\text{Cs}$ ,  $^{241}\text{Am}$ ,  $^{133}\text{Ba}$  produced by AEA Technology,  $^{24}\text{Na}$   $\gamma$ -ray source generated by the neutron activation  $^{27}\text{Al}(n, \alpha)^{24}\text{Na}$ , AmBe neutron source and the associated 4.438 MeV  $\gamma$ -ray from  $^{12m}\text{C}$  [11], and also the naturally occurring radioactivity from  $^{138}\text{La}$ . The non-proportionality response (nPR) was also studied using these  $\gamma$ -rays.

The fast neutron responses of  $^{79}\text{Br}$  and  $^{81}\text{Br}$  were investigated by using the DT reaction neutron. The CLLB crystal and aluminum housing as a whole were irradiated, energy spectrum of  $\gamma$ -ray emitted by the activated product and the half-life of the corresponding radionuclide were measured and analyzed based on a GEM60P HPGe detector. Furthermore, pulsed DT fast neutron source was used to investigate the 15 MeVee–18 MeVee high-energy events, and the influence of unexpected decay  $\gamma$ -rays emitted by  $^{78}\text{Br}$  and  $^{80}\text{Br}$  in experimental measurements.

### 3. Results and discussion

#### 3.1. The characteristics of CLLB

In this section, the pulse shapes for gamma-ray, alpha particle, thermal and fast neutron pulse shapes were derived. And then, the particle discrimination performance was investigated based on the waveforms. The gamma-ray response, energy resolution and intrinsic non-proportionality response were also investigated.

##### 3.1.1. Pulse shape discrimination performance

Pulse shapes for  $\gamma$ -ray, alpha particle, thermal and fast neutron events from CLLB are shown in Fig. 1, pulse height were normalized to 1. Each pulse is obtained averaging 25 pulses of approximately equal amplitude. The  $\gamma$ -ray events are from the 2754 keV  $\gamma$ -ray emitted by a  $^{24}\text{Na}$  radionuclide, alpha events are from the intrinsic background of the daughter nuclei from  $^{227}\text{Ac}$ , a contamination of the lanthanum component. Thermal and fast neutron events are from AmBe and DT reaction neutron sources, respectively. Pulse rise time from 10% of the maximum pulse amplitude to 90% is 24.3 ns for  $\gamma$ -ray event, while 22.1 ns for alpha and neutron events.

In terms of pulses generated by CLLB, electrons induced by  $\gamma$ -ray produce a slow decay component that has a greater ratio than the higher  $dE/dx$  particles [3]. Thermal neutron reacts with  $^6\text{Li}$  in the CLLB crystal to produce an alpha particle and a triton, and the waveform for thermal neutron is co-generated by both particles. Meanwhile, waveform for fast neutron event maybe generated by alpha, triton, deuteron, proton,

and/or co-produced by these particles which produced by fast neutron induced reactions. So we can see that the fast neutron generated waveforms are located between the waveforms of  $\gamma$ -ray and alpha particle.

Firstly, PSD performance for  $\gamma$ -ray and alpha particle was investigated by measuring the naturally occurring intrinsic background of the CLLB scintillator,  $\gamma$ -rays are mainly from  $^{138}\text{La}$  and natural background, while alpha particles are from the daughter nucleus of  $^{227}\text{Ac}$  as mentioned above. The PSD-PH 2D histogram, PH and PSD figures are shown in pad 1, pad 2, and pad 3 of Fig. 2. The measuring time is 2171 s.  $\gamma$ -rays and alpha particles can be separated easily and effectively using a simple curve as shown in pad 1, thus the PH spectra of  $\gamma$ -ray and alpha were obtained as shown in pad 2. The two distinct peaks in pad 2 (red line) are 778 keV and 1468 keV (the sum of  $\gamma$ -ray 1436 keV and X-ray 32 keV)  $\gamma$ -rays emitted by  $^{138}\text{La}$ . The FoM of  $\gamma$ -ray and alpha is 1.24 in the condition of  $12000 < PH < 40000$ .

Secondly, we use a moderated AmBe neutron source to investigate the PSD performance between thermal neutron and  $\gamma$ -ray with a radioactivity of  $\sim 10^6 \text{ s}^{-1}$ . Pulses were acquired directly by the DT5751 FADC with a lower threshold of 6 mV, the measured total events is equal to 224587. Results of PSD and PH performance are shown in Fig. 3.

As can be seen from pad 1 in Fig. 3, the cluster produced by thermal neutrons is located below the PSD line, while  $\gamma$ -ray events appear above the PSD line. The thermal neutrons induced peak (blue line) is clearly shown in pad 2, while the three peaks of  $\gamma$ -rays (red line) are 4438 keV from  $^{12m}\text{C}$ , single escape (SE) peak and double escape (DE) peak, respectively. The FoM between  $\gamma$ -ray and thermal neutron (also including a small quantity of fast neutron events) is equals to 1.23 in the condition of  $16000 < PH < 20000$ , the events is shown in the rectangle on pad 1 of Fig. 3.

##### 3.1.2. $\gamma$ -ray response and nPR

Gamma energy spectra of  $^{241}\text{Am}$ ,  $^{137}\text{Cs}$ ,  $^{24}\text{Na}$ , natural and intrinsic background, and that from AmBe source are shown in Fig. 4, the energy was obtained by integrating the time window of 1400 ns with the charge integration method. Three background  $\gamma$ -ray emission lines at 1461 keV from  $^{40}\text{K}$ , 1468 keV from  $^{138}\text{La}$  and 2614 keV from  $^{232}\text{Th}$  can be seen in the upper pad (black line).  $\gamma$ -ray peaks at 1368 keV and 2754 keV from  $^{24}\text{Na}$ , the SE and DE of the latter, and the summed peaks are shown as the purple line. However,  $^{241}\text{Am}$  and  $^{137}\text{Cs}$  energy spectra show only photopeak and superimposed on the  $^{24}\text{Na}$  energy spectrum. The  $\gamma$ -ray peak at 4438 keV from  $^{12m}\text{C}$  and the associated DE and SE, thermal neutron capture event with the electron equivalent energy deposit of 3229 keVee, are shown in the lower pad of Fig. 4.

Accordingly, energy resolution and the corresponding FWHM obtained for  $\gamma$ -rays are shown Fig. 5. Energy resolution was obtained using  $(\text{FWHM}/E_p) \times 100\%$ , where  $E_p$  is the energy of photopeak, energy resolution is 4.84% at 662 keV, which exhibits much better energy resolution than commonly used NaI crystal [12]. FWHM is described as Eq. (1) in the MCNP code [13] and the fitted curve is shown as the blue dash line in Fig. 5.

$$\text{FWHM} = a + b\sqrt{E} + cE^2 \quad (1)$$

Scintillators have an intrinsic non-proportionality response between scintillator light yield and photon deposition which affects their energy resolution. The origin of non-proportional response in scintillator is extremely complex, which can be affected by factors such as chemical composition, dopants, rare earth-cation substitution effect and anion effect and so on [14–16]. The nPR can be explained that it originates from the non-linear interactions of electrons and holes in a tiny excitation volume leading to a quenching of luminescence [16].

The  $\gamma$ -ray non-proportionality response can be traced back by means of experiment. Following the ideas of Pieter Dorenbos [17] and Wahyu Setyawan et al. [14], a nPR of  $\sim 2\%$  in the energy range from 59.6 keV to 4438 keV are shown in Fig. 6, all the points were normalized to 1

Download English Version:

<https://daneshyari.com/en/article/8165886>

Download Persian Version:

<https://daneshyari.com/article/8165886>

[Daneshyari.com](https://daneshyari.com)